CHEMICAL ENGINEERING TRANSACTIONS, Volume 12, 2007
Edited by Jiri Klemeš

Simulation of Phase Distributions during Freeze-drying through Pore-scale Network Modelling

Yongzhong Liu*, Hao Sun, Yanfei Zhao
Department of Chemical Engineering, Xi'an Jiaotong University
No.28 Xianning West Road, Xi'an, 710049, P. R. China

The primary objective of this work is to explore the evolution of the temperature profiles and the phase distributions during freeze-drying at pore level. A pore-throat network model for freeze-drying was proposed on the basis of pore size distribution of freeze-dried material, in which mass balance and energy balance equations were solved. The simulation results show that the predicted drying curve agrees well with the experimental data during the primary drying stage. It is capable of capturing the characteristics of the temperature profiles and the phase distributions at the pore level.

1. Introduction

Freeze-drying is an indispensable method to preserve substances that are heat-sensitive and/or oxygen-sensitive (Rey, 2004). Determining a transitional point distinguishing the primary drying from the secondary drying precisely has become an important issue in most practical operations when operating strategies are optimized. Although some direct/indirect measurement methods could be used for monitoring the process (Genin et al, 1996; Oetjen, 2004; Tang, et al, 2005), the determination of the end point of the primary drying is still largely empirical owing to diversity of material properties and operational parameters. It remains a challenge to judge the end point of the primary drying by a precise determination of the residual moisture in the material theoretically.

A pore-throat network model was proposed to simulate a freeze-drying process in this paper. The main objective of this work is to explore the evolution of phase distributions and temperature profiles during primary drying at pore level, which is of importance in determining the transitional point theoretically. The unique feature of the modelling is to take the micro-structural characteristics of the material of interest into consideration, to which is usually paid little attention in the conventional models.

2. A Pore-scale Network Model for Freeze-drying

2.1 A pore-throat network model to represent the freeze-dried material

In general, freeze-drying falls into three stages: freezing, primary drying and secondary drying. During the primary drying stage, the sublimation interface separates the slab into two zones with different nature, i.e. a dried zone and a frozen zone. A bundle of interwoven channels together with the solid skeleton of the material comprise the dried zone, and form a typical porous medium with a certain pore size distribution. Regarding the phase distributions related to the behaviors of heat and mass transfer during drying,

the micro-structural characteristics of the dried region should be engaged in the model at the first place. A pore-scale network model is in the position of incorporating the micro-structural characteristics into modeling.

A regular square pore-throat network can represent porous medium in a 2-D coordinate system (Prat, 2002). In freeze-drying, the characteristics of the porous structure of the dried zone in the material, such as pore size, shape and connectivity, are mainly dependent on the ice crystals formed in the freezing stage. In this regular network, nodes represent pores, while channels that connect two nodes, represent throats. In order to reproduce the randomness of throat size in nature, the actual pore size distribution of freeze-dried material is assigned to the throat in the network. In the network, the pore chambers are classified into three types according to the content inside the pore: frozen pore chamber (FPC), in which ice is filled; sublimation pore chamber (SPC), in which sublimation occurs, and gas pore chamber (GPC), in which gases mixture exists.

2.2 Mass and heat balance

Freeze-drying is a process in which heat and mass transfer are coupled in the dried zone and on the sublimation interface. Hence, mass and heat balance should be conducted to obtain the phase distributions and the temperature profiles within the material. Some assumptions are applied: (1)initially, a certain amount of ice that is equal to the initial moisture content of the material is assigned to the pore chambers, and the bound water in the material is ignored; (2) ice is solely in pore chambers and not in the throats; (3) the phase change instantaneously reaches the thermodynamic equilibrium when sublimation occurs; (4) gases mixture are ideal; (5) the primary drying terminates when ice disappears from all of the pore chambers in the network.

Mass balance for FPC, SPC and GPC should be implemented in the network as shown in Fig.1(a). For any FPC, the moisture content in the pore is constant and equals to the initial value. No mass changes in these pore chambers. Initially, the pores in the network are completely filled with ice. The partial pressure of vapor at the top edge of the network is equal to the saturated vapor pressure that is corresponding to the temperature of ice on the surface of coil in the vapor condenser. The other three edges of the network are impermeable walls. In the network model in this paper, the grid of the mass transfer network overlaps that of the heat transfer network.

(a) Mass transfer network *(b) Control volume of heat transfer*

Fig.1 Mass and heat transfer in the pore-throat network

In any GPC, the mass balance of the chamber can be written as

$$V_{i,j}\frac{c_{i,j}^{p+1}-c_{i,j}^{p}}{\Delta\theta}=F_{i-1,j}^{p}+F_{i+1,j}^{p}+F_{i,j-1}^{p}+F_{i,j+1}^{p} \tag{1}$$

where $c_{ij}=P_{ij}/RT_{ij}$ stands for the vapor concentration in the pore chamber; P stands for the partial pressure of vapor in the GPC; F stands for the mass flow rate of vapor in a throat that connects two neighboring chambers. Δθ is time step. The subscripts (i-1, j), (i+1,j), (i, j-1) and (i, j+1) denote the chambers that are immediately adjacent to the pore chamber (i, j) .

In any SPC, the moisture content in the pore is made up of vapor and ice. Within each time step, the variation of ice amount in each SPC can be written as a function of ice saturation in pore chamber

$$V_{pore}\rho_{ice}\frac{\varphi_{i,j}^{p+1}-\varphi_{i,j}^{p}}{\Delta\theta}=\frac{\Delta M_{ice}}{\Delta\theta}=F_{i-1,j}^{p}+F_{i+1,j}^{p}+F_{i,j-1}^{p}+F_{i,j+1}^{p} \tag{2}$$

where φ is a variable that indicates the status of SPC, which is defined as $\varphi=V_{ice}/V_{pore}$.

The vapor flow rate in any throat connecting two neighbor pores, F_{ab}, is calculated by

$$F_{ab}=D_{ab}A_{ab}(P_a-P_b)/(RTl) \tag{3}$$

where P_a and P_b are the vapor pressures in the adjacent pores a and b, respectively. D_{ab} is the vapor diffusion coefficient at the local temperature T. A_{ab} is the cross section area of the throat. If phase change occurs in the pore, the saturated vapor pressure is used. It is assumed that mass transfer only takes place within the throats, which are perceived as capillary tubes. For freeze-drying foodstuff, vapor diffusion could be considered Knudsen flow when $Kn>2$. The vapor flow falls into the continuum regime when $Kn<0.01$. When $0.01<Kn\le 2$, the vapor flow lies in the transitional flow regime (Hill & Sunderland, 1971). In the continuum flow regime, the diffusivity of the vapor in the binary gas mixture, D_{av}, can be estimated by the Hirschfelder-Curtiss-Bird equation (Bird, 1960). In the case of Knudsen flow, the diffusivity D_{kv} can be calculated by Knudsen diffusion. For the diffusion coefficient in the transitional flow regime D_{tv}, the combination of continuum flow and Knudsen diffusion is adopted (Geankoplis, 1993).

As regard to heat balance, the control volume in the heat transfer network is shown in Fig. 1(b). The energy balance is carried out on the control volume, written as

$$\rho_k C_{Pk}\Delta V\left(\frac{T_{i,j}^{p+1}-T_{i,j}{}^{p}}{\Delta\theta}\right)=\Phi_{i-1,j}^{p}+\Phi_{i+1,j}^{p}+\Phi_{i,j-1}^{p}+\Phi_{i,j+1}^{p}+\Delta H_s W_{water}\left(\frac{\Delta M_{ij}}{\Delta\theta}\right) \tag{4}$$

$$\Phi_{i-1,j}=\lambda_k\Delta A(T_{i-1,j}-T_{i,j})/l+F_{i-1,j}W_{water}C_{pg}(T_{i-1,j}-T_{i,j})$$

$$\Phi_{i+1,j}=\lambda_k\Delta A(T_{i+1,j}-T_{i,j})/l+F_{i+1,j}W_{water}C_{pg}(T_{i+1,j}-T_{i,j})$$

$$\Phi_{i,j-1} = \lambda_k \Delta A (T_{i,j-1} - T_{i,j}) / l + F_{i,j-1} W_{water} C_{pg} (T_{i,j-1} - T_{i,j})$$
$$\Phi_{i,j+1} = \lambda_k \Delta A (T_{i,j+1} - T_{i,j}) / l + F_{i,j+1} W_{water} C_{pg} (T_{i,j+1} - T_{i,j})$$

where Φ is the heat transfer rate; l is the grid width of the heat transfer network, which equals the distance between two adjacent pores; ΔV and ΔA are the control volume and the control surface, respectively; $\Delta M_{ij}/\Delta\theta$ is the accumulation term of vapor in the SPC; W_{water} is the molar weight of water; C_p and λ_k are respectively heat capacity and thermal conductivity of the control volume, which depend on the location of the node.

In the modeling of a freeze-drying process by the pore-throat network model with coupled heat and mass transfer, equations listed above make up of a set of linear algebric equations that involves each node in the network. To obtain the solution to the problem, at first, the configuration of the pore-throat network should be constructed in terms of the pore size distribution of the material of interest. Thereafter the simulations of the drying process can be performed on the network under a certain operating condition of freeze-drying. In this work, all calculations were coded in MATLAB.

3. Results and Discussion

3.1 Validation of the model and the influence of network parameters on the simulation

To validate the presented model, a comparison between the experimental data in literature and the predicted drying curves of freeze-drying turkey was made. The properties of the model material are from Litchfield's work (1982). The operation conditions in the simulations are from Sandall's work (1967).

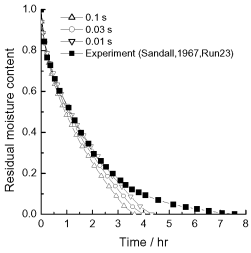

Fig.2 Comparison with the simulation result and the experimental data

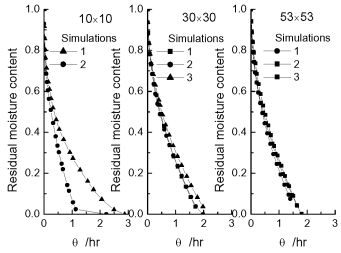

Fig.3 The influence of the network size on the simulations

Fig.2 shows the experimental drying curve for freeze-drying turkey (Run 23 in Sandall, 1967) along with the simulation results with different time step. The time steps chosen in the simulations are 0.1, 0.03, and 0.01s, respectively.

It is shown that the simulations agree well with the experimental data before 80% water is removed from the material. The deviation of the drying curve below 20% of the residual moisture content is mainly because the desorption was not taken into account in the model. It is observed in the original experimental data that after 80% of water is

removed, the secondary drying stage begins, in which desorption regins. With reducing the time step in the simulation, the predicted drying curves are in a good agreement with the experimental data. However, smaller time step require much more computation efforts for a certain network. In these simulations, the network size is 30 by 30. For example, for the time step 0.01s, it takes more than 400 hours for the calculation.

The size of the pore-throat network is an important parameter for representing the micro-structure of the material in the simulations. Fig.3 shows the influence of the network size on the simulations. 10×10, 30×30 and 53×53 were chosen in the simulations. The results show that when the size of the network is smaller, larger deviation of the drying curves exists in the different simulations. While the size of the network is larger, not much difference among the drying curves is observed. As shown in the figure, it is appropriate to choose 30×30 as the size of the network in the simulations to trade off the accuracy of the model for the computational hours.

3.2 The evolution of temperature profiles and phase distributions during drying

The primary advantage of the pore-throat network model is the capabilities of capturing the temperature profiles and the phase distributions in the pore level. Fig.4(a) and 4(b) shows the evolution of the temperature profiles and the phase distributions during drying predicted by the model in the order of the residual moisture content of the material during the drying, respectively. It is shown that the isotherms within the upper part of the material are much denser than those within the lower part of the material during the whole drying process. This implies that there exists a larger temperature gradient within the dried zone than that of the frozen zone. The isotherms become gradually sparse as drying progresses. In addition, the isotherms close to the frozen zone are more irregular than those near the open edge of the network. The isotherm that is close to the sublimation pores delineates the pattern of the drying front. Obviously, the irregular shape of the drying front reflects that the retreating rate of the front is different from point to point because of the pore size distribution in the dried zone. It is worth of noting that there are some closed isotherms in the material at the earlier stage of the

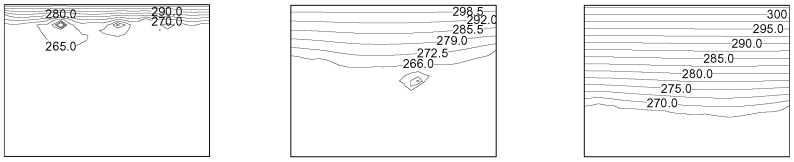

(a) The evolution of temperature profiles

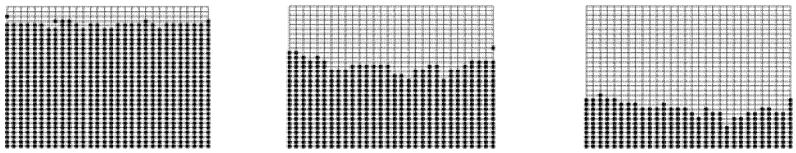

(b) The evolution of phase distribution

Fig. 4 Temperature profiles and phase distributions in the course of drying

drying process, which are near the sublimation interface in the material. Their sites correspond to the concave positions of the interface, as shown in Fig.4 (b). The temperatures at these sites are lower than that of their neighbors owing to a larger sublimation rate and mass transfer rate.

Fig.4(b) shows the phase distributions within the material during drying. In the figures, the black square blocks in the network represent the pores that are occupied by ice, while the grid intersections are the pores that are filled with gases. It can be seen from Fig.4 (b) that the patterns of the sublimation front are irregular and different from the smooth flat or curving surface that could be predicted by the convetional continuum models. During drying, the invasion of gases mixture into the frozen zone results in the irregular drying front, and some moisture patches remain in the network. The main reason for the patterns of the phase distribution is that mass transfer flux is imbalance throughout the network due to the stochastic distribution of throat sizes.

4. Conclusions

A 2-D pore-throat network model for the primary drying stage of freeze-drying was proposed. The unique feature of the modeling is to investigate the behaviors of drying dynamics, such as the phase distributions and the temperature profiles, at the pore scale. The results show that reducing the time step and enlarging the network size in the simulation lead to the improvement of the accuracy of the model, but much computation effort is required. Therefore, it is crucial to choose the size of the network and the time step in the simulation in order to acquire a reasonable accuracy of the prediction within tolerable computational hours. The simulations will provide insights into the quality control of product and theoretical approach for reducing the risk of drying failure.

5. References

Bird, R.B., W.E. Stewart, E.N. Lightfoot, 1960, Transport phenomena. John Wiley & Son, Inc. New York

Geankoplis, C. J., 1993, Transport processes and unit operation, Prentice Hall P T R, New Jersey

Genin, N., F. Rene, G. Corrieu, 1996, Chemical Engineering & Processing, 35, 255

Hill, J.E., J.E. Sunderland, 1971, Int. J. of Heat Mass Transfer 14, 625.

Litchfield, R.J., A.I. Liapis, 1982, Chem. Engng. Sci. 37, 45

Oetjen, Georg-Wilhelm, P. Haseley, 2004, Freeze-drying, Wiley-VCH Verlag Gmbh & Co. Weinheim

Prat, M., 2002, Chemical Engineering Journal 86, 153.

Rey, L., J.C. May, 2004, Freeze-drying/Lyophilization of pharmaceutical and biological products, Marcel Dekker Inc., New York

Sandall, O.C., C.J. King, C.R.Wilke, 1967, AIChE J 13, 428

Tang, Xiaolin, S.L. Nail, M.J. Pikal, 2005, Pharmaceutical Research 22, 685

Acknoledgements

The authors gratefully acknowledge the financial support by the Natural Science Foundation of China (NSFC), Grant No.20206026 and Grant No. 20436040.